Transcript profiling reveals the role of PDB1, a subunit of the pyruvate dehydrogenase complex, in Candida albicans biofilm formation

Laxmi Shanker Rai, Murielle Chauvel, Emmanuelle Permal, Christophe D'Enfert, Sophie Bachellier-Bassi

Original Article

Transcript profiling reveals the role of *PDB1,* a subunit of the pyruvate dehydrogenase complex, in *Candida albicans* biofilm formation

Laxmi Shanker Rai [a], Murielle Chauvel [a], Emmanuelle Permal [b], Christophe d'Enfert [a], Sophie Bachellier-Bassi [a], *

[a] *Institut Pasteur, Université Paris Cité, INRAE, USC2019, Unité Biologie et Pathogénicité Fongiques, F-75015 Paris, France*
[b] *Institut Pasteur, Université Paris Cité, Hub de Bioinformatique et Biostatistique, F-75015 Paris, France*

A R T I C L E I N F O

A B S T R A C T

Candida albicans, the most prevalent fungal pathogen in the human microbiota can form biofilms on implanted medical devices. These biofilms are tolerant to conventional antifungal drugs and the host immune system as compared to the free-floating planktonic cells. Several *in vitro* models of biofilm formation have been used to determine the *C. albicans* biofilm-forming process, regulatory networks, and their properties. Here, we performed a genome-wide transcript profiling with *C. albicans* cells grown in YPD medium both in planktonic and biofilm condition. Transcript profiling of YPD-grown biofilms was further compared with published Spider medium-grown biofilm transcriptome data. This comparative analysis highlighted the differentially expressed genes and the pathways altered during biofilm formation. In addition, we demonstrated that overexpression of the *PDB1* gene encoding a subunit of the pyruvate dehydrogenase resulted in defective biofilm formation. Altogether, this comparative analysis of transcript profiles from two different studies provides a robust reading on biofilm-altered genes and pathways during *C. albicans* biofilm development.

1. Introduction

Biofilms are three-dimensional microbial communities, within which individual cells are protected against diverse environmental insults, such as immune cells or antimicrobial drugs [1–3]. *Candida albicans* is a fungal commensal of the human microbiota causing both superficial and systemic infections. *C. albicans* forms biofilms on a variety of tissues and medical devices introduced in the host including intravascular catheters [4–6]. *C. albicans* biofilms are structured and consist of differentiated cell types including yeast, pseudo-hyphae and hyphae, which are encased in a self-generated extracellular matrix [7–9]. These biofilms are tolerant to conventional antifungal drugs as compared to the free-floating planktonic cells, due to an entrapment effect of the extracellular matrix and the up-regulation of drug efflux pumps [10–12]. In the first phase of *C. albicans* biofilm development, cells adhere to solid surfaces and proliferate, forming a basal layer that is commonly composed of yeast cells. Then, these basal layer cells differentiate into distinct cell types including pseudo hyphae and hyphae that contribute to the final architecture of the biofilm and produce a protective extracellular matrix mainly composed of polysaccharides and proteins [13,14]. Finally, yeast cells are released from this complex structure with the possibility to seed at new sites [9,15,16]. In the laboratory, *C. albicans* biofilm formation can be assayed in several models, either *in vitro* on different surfaces including silicone squares or polystyrene microtiter plates, or *in vivo* on catheters or dentures placed in the rat [17–19]. Different media and experimental conditions have been utilized to decipher the properties of *in vitro*-grown *C. albicans* biofilms. Indeed, *C. albicans* can efficiently form biofilms in Spider, RPMI, YPD (yeast extract-peptone-dextrose), and YNB (yeast nitrogen base) media [20–23]. However, the extent of biofilm formation varies with the condition used [22]. Over the past years, genetic networks regulating biofilm development have been studied, using both *in vitro* and *in vivo* models [20,24,25]. Genomic approaches have been used to identify differentially expressed genes during *C. albicans* biofilm growth [25–28]. Other studies have uncovered the role of glycolysis and tricarboxylic acid (TCA) pathway during *C. albicans* biofilm

formation and highlighted the alteration of metabolic activities during this mode of growth [24,29,30].

Here, we used an RNA sequencing approach to identify differentially expressed genes and altered pathways when *C. albicans* forms biofilms in YPD medium, as compared to planktonic cells. This YPD-grown biofilm transcriptome set of data was further compared with a previously published transcriptome data obtained from Spider medium-grown biofilms [25]. The overlap of genes differentially expressed in both datasets gave information about pathways altered during *C. albicans* biofilm formation regardless of the environmental conditions. As previously shown [29], we observed that genes involved in amino acid metabolism are up-regulated whereas genes of the TCA cycle are down-regulated during biofilm formation. We also demonstrated that over-expression of *PDB1*, encoding a subunit of the pyruvate dehydrogenase complex acting as a bridge between the glycolytic and the tricarboxylic acid pathways, impairs both filamentation on solid medium and biofilm formation. We propose that this comparative gene expression analysis provides robust information about biofilm differentially expressed genes and the pathways altered during *C. albicans* biofilm formation.

2. Results

2.1. C. albicans *forms efficient biofilms in YPD medium*

In this study, we grew *C. albicans* biofilms in YPD medium, commonly used for yeast growth. Free-floating cells were allowed to adhere to silicone squares and biofilms were grown in YPD medium at 37 °C for 18 h. The biofilms developed on the silicone surface were examined by confocal laser scanning microscopy (CLSM). In such conditions, the wild-type reference strain CEC4665 developed robust biofilms (Fig. 1, left panel). To validate our experimental conditions, we tested the involvement of key biofilm regulators, namely Tec1 and Ndt80, that had been identified in studies relying on Spider medium-grown biofilms [25]. We also tested a strain deleted for *UME6*, which has been shown to be important for biofilm formation in the reference strain SC5314 grown in RPMI [28]. We compared the biofilm-forming ability of *tec1Δ/tec1Δ*, *ndt80Δ/ndt80Δ* and *ume6Δ/ume6Δ* null mutant strains to the wild-type strain. CLSM results confirmed that unlike the wild-type strain, null mutants of *TEC1*, *NDT80* and *UME6* were defective in biofilm formation when grown in YPD medium (Fig. 1). Thus, we showed that the function of these biofilms key regulators remains unchanged when biofilms are grown in YPD medium.

2.2. *Transcript profiling of* C. albicans *biofilms in YPD*

To identify genes differentially expressed during *C. albicans* biofilm growth in YPD medium, we performed a genome-wide transcriptome study with wild-type *C. albicans* planktonic and biofilm cells grown in this medium. A total of 1634 genes were up-regulated (log$_2$ fold change >1.2 with P < 0.05) whereas 1331 genes were down-regulated (log$_2$ fold change < -1.2 with P < 0.05) during *C. albicans* biofilm formation as compared to the planktonic cells (**Datasheets S1A and S1B**). These differentially expressed genes were functionally categorized in order to pinpoint the pathways modulated during the course of *C. albicans* biofilm formation. Genes up-regulated during transition from planktonic to biofilm formation (i.e. biofilm induced genes) pertained to cellular metabolism. The metabolic pathways significantly altered during this transition include metabolism of carbohydrates (starch, sucrose, and galactose), lipids (fatty acids and alpha-linolenic acid), nitrogen and amino acids (arginine,
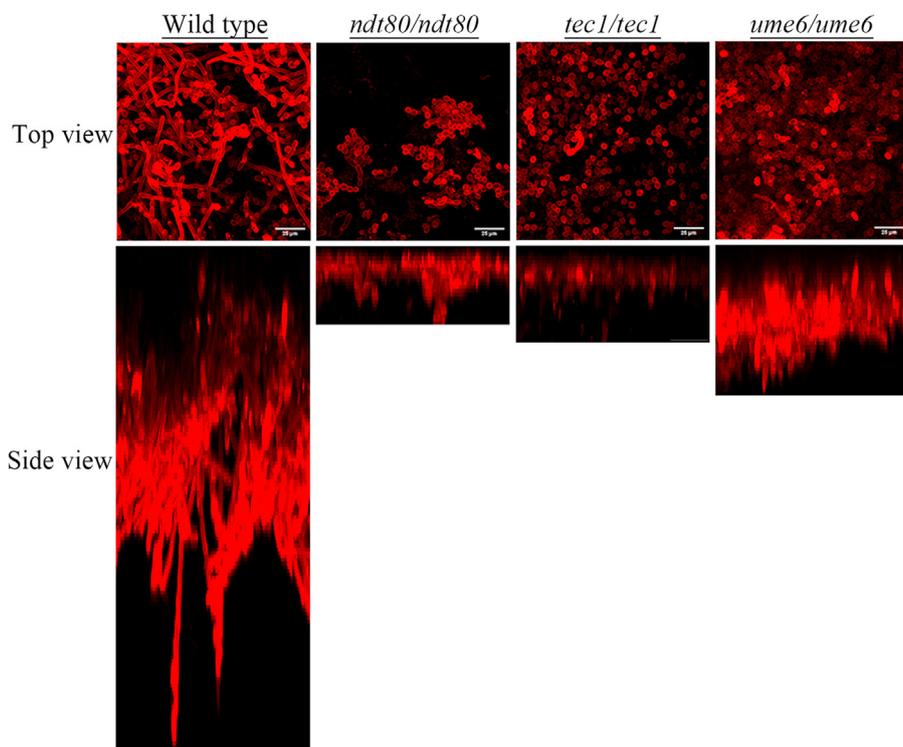
Fig. 1. *C. albicans* biofilm formation in YPD medium. Biofilms formed by *C. albicans* wild-type (CEC4665), and the null mutant strains *ndt80Δ/ndt80Δ* (CJN2412), *tec1Δ/tec1Δ* (CEC3589) and *ume1Δ/ume6 Δ* (CEC3583) grown on silicone squares in sterile 12-well plates in YPD medium at 37 °C for 18 h. The wells were washed with 1× PBS to remove non-adherent cells. Biofilms were stained with concanavalin A-Alexa 594 and imaged by CLSM. Images are projections of the top and side views. Scale bars: 25 μm.

proline, alanine, aspartate and glutamate, phenylalanine, valine, leucine isoleucine and taurine). ABC transporters were also significantly up-regulated in *C. albicans* biofilm cells as compared to planktonic cells (Fig. 2A). The altered pathways' details and their *p*-values are given in **Datasheet S1C**. Similarly, a pathway analysis was performed for *C. albicans* biofilm down-regulated genes. It showed that ribosome, oxidative phosphorylation, biosynthesis of secondary metabolites, carbon metabolism, citrate cycle (TCA cycle), protein processing in endoplasmic reticulum, and steroid biosynthesis were significantly altered (Fig. 2B). The details altered pathways details and their *p*-values are given in **Datasheet S1D**. Thus, based on pathway analysis of biofilm differentially expressed genes, we conclude that the major changes that occur when *C. albicans* cells shift from solitary to community mode of growth in YPD medium affect cellular metabolism including alteration of the respiratory behavior.

2.3. Comparison of transcript profiles of spider- and YPD-grown C. albicans biofilm

It has been shown previously that *C. albicans* biofilm architecture and properties vary with the media used [22]. Therefore, we were interested in determining the common set of genes altered during *C. albicans* biofilm formation irrespective of the growth conditions. We thus performed a similar pathway analysis on a previously published Spider-induced biofilm transcriptome set of data [25]. In that study, a total of 1734 genes were up-regulated (log2 fold change >1 with $P < 0.05$) and 760 genes were down-regulated (log2 fold change < -1 with $P < 0.05$) as compared to planktonic cells. Pathway analysis showed that most up-regulated genes during *C. albicans* biofilm formation in Spider medium are linked to the cellular metabolism. Metabolism of carbohydrates, amino acids (arginine proline, alanine, aspartate, glutamate, and
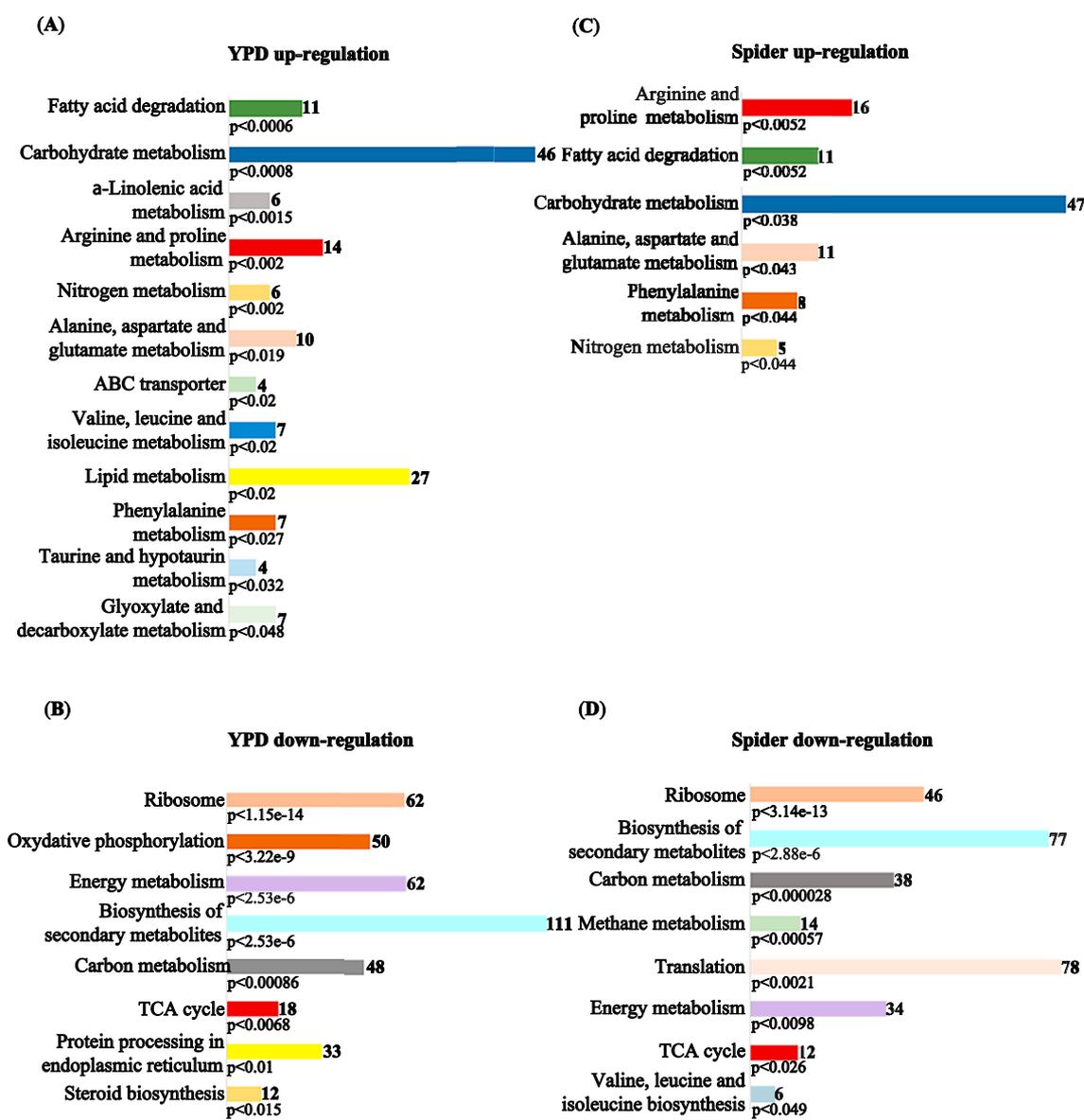
Fig. 2. Transcriptome profiling of *C. albicans* biofilm grown in YPD and Spider media. A global gene expression study was performed with total RNA isolated from wild-type (CEC4665) cells grown in planktonic or biofilm conditions in YPD medium. KEGG analysis was performed for the functional classification of (**A**) up and (**B**) down-regulated genes using FungiFun2 [53]. A similar pathway analysis was performed with a previously published study [25] where biofilm was grown in Spider medium. Functional classification of (**C**) up-regulated and (**D**) down-regulated genes.

phenylalanine) and nitrogen, as well as fatty acid degradation were the most significantly altered pathways (Fig. 2C). On the other hand, down-regulated genes were linked to ribosome, translation, metabolism of carbon, carbohydrates, methane, TCA cycle, and biosynthesis of secondary metabolites (Fig. 2D). The altered pathways' details and their *p*-values are given in **Datasheets S1E** and **S1F**. Comparison of transcriptome analysis of planktonic and biofilm cells obtained from these two different studies suggested that the shift from planktonic- to biofilm-mode of growth induces a major change in cellular metabolism regardless of the growth medium.

We then compared the global gene expression profile obtained from two different biofilm- forming conditions, i. e. YPD and Spider media. The comparison of these two genome-wide studies revealed that 1010 (42.6%) of the up-regulated genes and 464 (28.5%) of the down-regulated genes are common between the two sets of data (Fig. 3A, Datasheet S1G and **S1H**). These results also suggested that a fraction of altered gene sets was specific to the environmental conditions used to isolate planktonic and biofilm cells. Next, we considered the genes common to both studies to determine the altered pathways during *C. albicans* biofilm formation. Functional categorization of common up-regulated genes between Spider or YPD grown biofilms suggested that amino acid metabolism (arginine and proline metabolism, alanine, aspartate and glutamate metabolism and phenylalanine metabolism), carbohydrate

metabolism, fatty acid degradation, nitrogen metabolism, and ABC transporters are the significantly altered pathways (Fig. 3B and **Datasheet S1I**). Similarly, functional categorization of down-regulated genes common to both Spider- and YPD-grown biofilms as compared to planktonic cells was carried out. This analysis revealed that genes belonging to protein synthesis (ribosome and translation), carbon metabolism, biosynthesis of secondary metabolites, methane metabolism and citrate cycle (TCA cycle) are repressed (Fig. 3C). Details of the altered pathways and their *p*-values are given in **Datasheet S1J**. This analysis with two different genome-wide datasets provides a robust information on *C. albicans* core genes that are differentially expressed during biofilm formation, as well as the altered pathways.

2.4. Overexpression of pyruvate dehydrogenase subunit PDB1, results in a defective biofilm

Earlier studies have shown an elevated transcription rate of the genes belonging to the glycolytic pathway during *C. albicans* biofilm formation [24]. In contrast, metabolomic studies of cells from planktonic and biofilm cultures have shown a lower accumulation of intermediates in the TCA cycle, namely citrate, fumarate, malate, and succinate during biofilm formation [29]. This is likely due to the diminished flux through the tricarboxylic acid cycle because the rate of aerobic respiration is low in biofilm cells [31]. Our
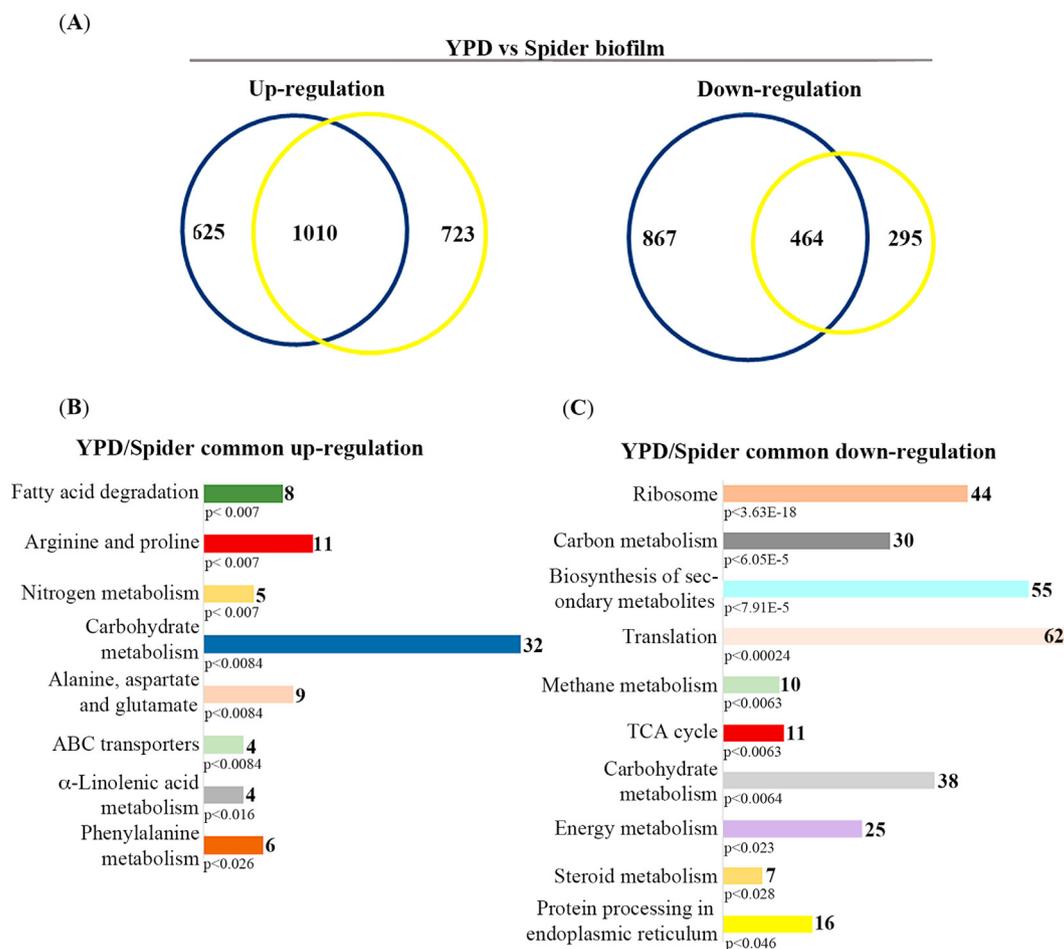
Fig. 3. Comparison of gene expression data of Spider and YPD-grown biofilms. (**A**) YPD- and Spider-grown biofilms genome-wide expression data were compared for genes that are altered in both biofilm growing conditions (blue and yellow circles, respectively) and represented as Venn diagrams. A total of 1010 up-regulated and 464 down-regulated genes are common between these two datasets. (**B**) KEGG analysis was performed for functional categorization for genes altered in the two studies using FungiFun2. Left panel: common up-regulated genes; right panel: common down-regulated genes.

comparative analysis of two genome-wide expression studies on *C. albicans* planktonic and biofilm cells showed that 11 genes belonging to the tricarboxylic-acid pathway as well as genes encoding pyruvate dehydrogenase were down-regulated in both datasets (Fig. 4A). Therefore, we examined the role of genes of the tricarboxylic-acid pathway components and of the pyruvate de-hydrogenase during *C. albicans* biofilm formation. To this aim, we utilized a doxycycline-dependent (P$_{TET}$) overexpression approach [32,33] and successfully constructed 7 strains allowing the doxycycline-dependent conditional overexpression of *PDA1* and *PDB1* (encoding two sub-units of pyruvate dehydrogenase), *MDH1-1* (malate dehydrogenase), *IDP1* (isocitrate dehydrogenase), *IDH2*

(NAD-isocitrate dehydrogenase), *LSC1* (putative succinate-CoA ligase) and *KGD2* (putative dihydrolipoamide S-succinyltransfer-ase). The biofilm assay was performed with the wild-type reference strain and the seven P$_{TET}$-driven overexpression strains both in the presence or absence of doxycycline. The extent of biofilm formation was measured by quantifying the biofilm dry mass. *PDB1* was the only gene among the seven candidate genes tested whose over-expression yielded a biofilm with a significantly reduced dry mass as compared to either the reference strain or the uninduced con-dition (Fig. 4B). To test if the reduction in biofilm formation is due to a general growth defect upon overexpression, we measured the growth rate of the wild-type parental strain and *PDB1*
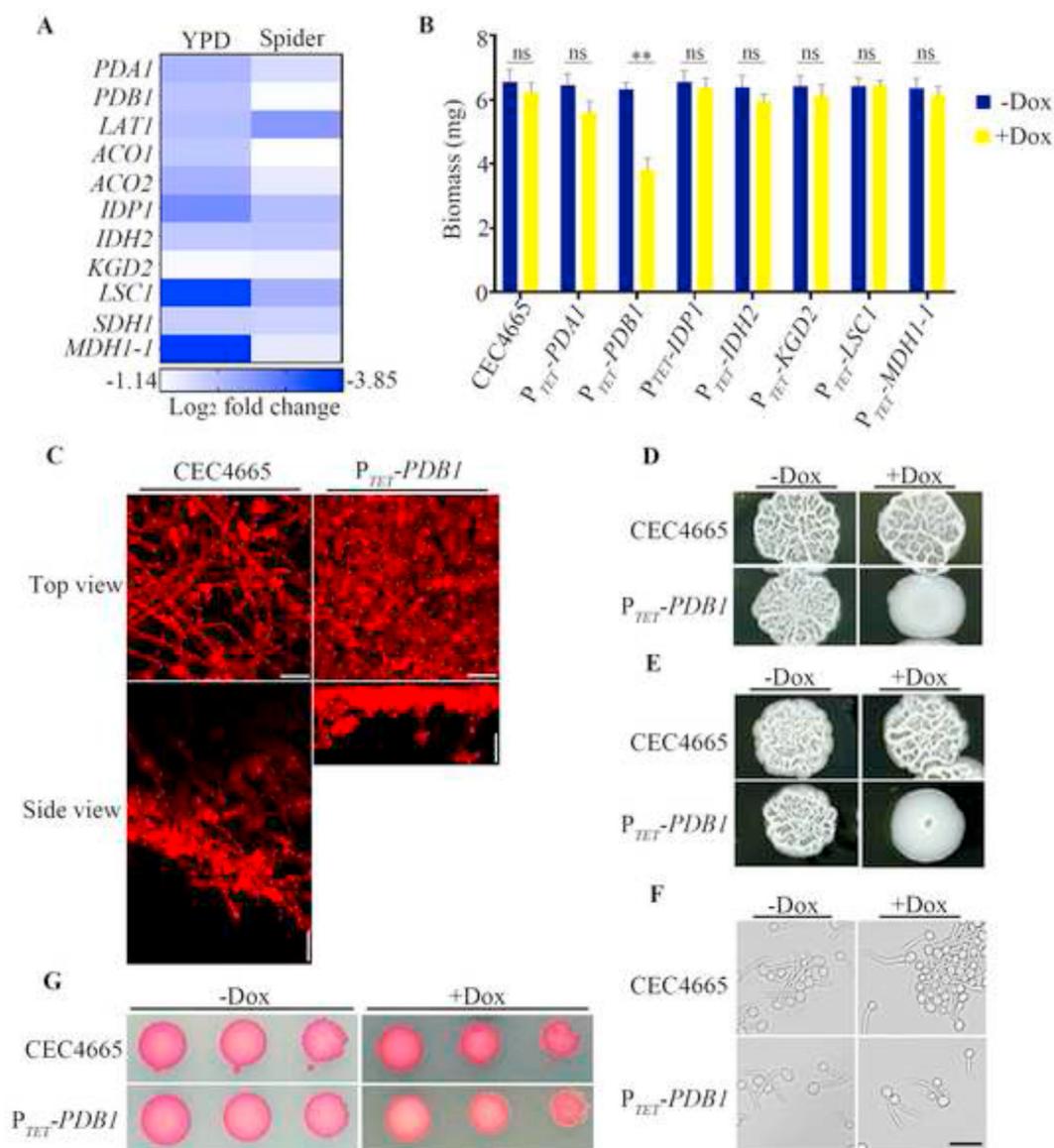

Fig. 4. *C. albicans PDB1* overexpression leads to form a defective biofilm. (**A**) A heat-map was generated for YPD and Spider common down-regulated genes related to the tricarboxylic acid pathway. (**B**) Dry weight of the wild-type (CEC4665) and overexpression strains of candidate genes examined for their ability to form biofilm with or without 40 μg/ml doxycycline. Multiple *t*-test were performed to find the statistical significance between uninduced and induced data sets. Padj value for P$_{TET}$-*PDB1* is 0.004 whereas as wild-type or other genes examined were not significant upon overexpression. (**C**) Wild-type (CEC4665) and P$_{TET}$-*PDB1*, strains were allowed to adhere to silicone squares in 12-well polystyrene plate in YPD medium supplemented with 40 μg/ml doxycycline at 37 °C for 1h; biofilms were grown for 18 h at 37 °C, stained with concanavalin A-Alexa 594 and imaged by CLSM. Images are projections of the top and side views. Scale bars: 25 μm. The extent of filamentation of wild-type (CEC4665) and P$_{TET}$-*PDB1* strains was estimated either by spot assay (**D**) or at the level of single colony (**E**) on YPD plates containing 20% fetal bovine serum with or without 40 μg/ml doxycycline incubated at 37 °C for 3 days. (**F**) Similarly, filamentation assay was performed in liquid YPD medium with 10% FBS for the indicated strains in the absence or presence of 40 μg/ml doxycycline at 37 °C. Scale bars: 25 μm. (**G**) Wild-type and P$_{TET}$-*PDB1* strains were spotted on YPD solid medium and allowed to grow with or without 40 μg/ml doxycycline at 30 °C for 24h. Cells were covered with a 0.025% TTC-agarose solution and pictures were taken after 30 min.

overexpression strain grown in liquid medium with or without doxycycline. We did not observe a significant growth difference upon overexpression of *PDB1,* showing that reduction in biofilm formation is not due to a growth defect (Fig. S1A). We also examined the growth pattern of P$_{TET}$-*PDB1* on solid YPD medium in the presence or absence of doxycycline (Fig. S1B). Again, we did not observe a significant growth difference upon overexpression of *PDB1*. To determine the structure and thickness of biofilms formed by the *PDB1* overexpression strain, confocal laser scanning microscopy (CLSM) was performed on biofilms grown in the presence of doxycycline. The CLSM observations further confirmed a reduction in the biofilm thickness upon *PDB1* overexpression as compared to the wild-type reference strain (Fig. 4C, side view).

2.5. Filamentation behavior of PDB1 *in the absence or presence of doxycycline*

Reduction in biofilm formation can be linked to a defect in filamentation, as described for *tec1* knock-out mutants for instance [10], and the top view of the biofilm formed upon *PDB1* overexpression contained mostly yeasts (Fig. 4C, top view). To determine whether the biofilm defect observed upon overexpression is caused by an alteration of filamentous growth, we examined the phenotype of the *PDB1* overexpression strain grown in hypha-inducing conditions in the absence or presence of doxycycline. Filamentation assays were performed on YPD medium containing fetal bovine serum (FBS) ± 40 μg/ml doxycycline, both by spotting assay and plating, to evaluate the phenotype at the single colony level. After 3 days at 37 °C, we observed that *PDB1* overexpression resulted in a defective filamentation on solid medium (Fig. 4D and **E**). Filamentation behavior of the *PDB1* overexpression strain was also monitored in liquid YPD medium containing FBS, with or without doxycycline. In liquid medium, the strain was able to grow as filaments even upon doxycycline-dependent *PDB1* induction (Fig. 4F). Thus, a filamentation defect specific to growth on a solid substrate may explain the biofilm reduction observed upon *PDB1* overexpression.

Next, we determined the mitochondrial activity upon overexpression of *PDB1* by using triphenyl tetrazolium chloride (TTC), a dye indicative of mitochondrial activity, as TTC reduction via the electron transport chain allows accumulation of the red pigment formazan within the cell [34]. The stable formation of formazan occurs strictly in anaerobic conditions. To monitor changes in mitochondrial activity upon *PDB1* overexpression, the wild-type and P$_{TET}$-*PDB1* strains were grown over-night either in the absence or presence of doxycycline and spotted on YPD plate with or without doxycycline. The TTC assay was performed after 24h of growth. Interestingly, we observed that overexpression of *PDB1* resulted in the production of a lighter color as compared to either the wild-type or uninduced conditions (Fig. 4G), indicating a reduced mitochondrial activity. This suggested that impaired biofilm formation and morphogenesis exhibited by the overexpression mutant could be linked to the creation of a hypoxic environment. Taken together, we report a role of the pyruvate dehydrogenase subunit *PDB1* in metabolic remodeling during *C. albicans* biofilm development.

3. Discussion

In this study, we performed a genome-wide transcriptome profiling on *C. albicans* cells grown either in planktonic or biofilm condition in YPD medium, and analyzed the functional categories differentially expressed during this growth transition. We then performed a comparative analysis between the set of genes differentially expressed in YPD-grown biofilms and a previously

published Spider-grown biofilm transcriptome data [25]. This comparative analysis allowed to highlight genes whose differential expression is important for biofilm formation regardless the environmental conditions, and confirmed previous findings, namely the up-regulation of genes involved in amino acid biosynthesis and down-regulation of genes involved in the TCA cycle. In addition, we demonstrated the role of the pyruvate dehydrogenase subunit Pdb1 in *C. albicans* biofilm formation.

Metabolic remodeling is one of the major changes occurring during microbial biofilm formation [26,27,29,30,35,36]. Garcia-Sanchez et al. (2004) utilized different growth conditions including nutrient flow, aerobiosis or glucose concentration and performed a transcriptome study to identify a core set of genes altered during *C. albicans* biofilm growth [26]. These authors observed that amino acid biosynthetic pathway genes are up-regulated during biofilm formation under aforementioned growth conditions. This led to the demonstration of the central role in biofilm formation of *GCN4*, a gene encoding a master regulator of amino acid biosynthetic genes in *C. albicans* [26]. The *gcn4Δ/gcn4Δ* null mutant strain produced a biofilm with a reduced biomass as compared to the wild-type cells, further confirming the role of amino-acid metabolism during *C. albicans* biofilm formation. In a similar study, Yeater et al. (2007) also observed the up-regulation of genes of the amino-acid biosynthesis during *C. albicans* early biofilm formation [27]. Further, it has been reported recently that the amino acid permease Stp2 is important in adherence and biofilm maturation [36]: *stp2* knock-out mutants are impaired for amino acid uptake and compensatory mechanisms in nutrient acquisition. This study also showed that a balanced amino acid homeostasis is critical for *C. albicans* biofilm formation. In addition, emerging data have suggested the role of arginine metabolism in *C. albicans* biofilm formation [30]. Interestingly, in our comparative study, we also observed that genes involved in arginine and proline biosynthesis (*ARG1, ARG3, ARG4, ARG5,6, ECM42, ORF19.5862, GDH2, PUT2* etc.), alanine, aspartate and glutamate biosynthesis (*GLN1* etc.) and genes involved in phenylalanine metabolism (*ARO9, HPD99* etc.) are being up-regulated during biofilm growth. Considering the fact that the rate of TCA cycle is low during biofilm formation, perhaps these amino-acids participate in the synthesis of protein products which may contribute to the extracellular matrix and are thus important for biofilm stability and cohesion. Further studies will reveal the contribution of these amino-acid biosynthetic genes during the *C. albicans* biofilm formation.

Bonhomme et al. (2011) observed the up-regulation of genes of the glycolytic pathway during *C. albicans* biofilm formation and highlighted the role of the transcription factor *TYE7* in their regulation [24]. They also investigated the establishment of a local hypoxic environment during *C. albicans* biofilm formation [24] and this was further established by measuring the oxygen level from top to bottom of the biofilms [37]. Another study comparing differentially expressed genes during biofilm formation and hypoxic environment in the closely related species *Candida parapsilosis* highlighted the alteration of expression of 60 genes induced in hypoxic environment and during biofilm formation [38]. Moreover, metabolomic study comparing *C. albicans* planktonic and biofilm cells uncovered differential production of metabolites mainly involved in the TCA cycle, lipid synthesis, amino-acid metabolism, glycolysis, and oxidative stress [29]. Interestingly, our comparative study also highlighted the down-regulation of genes whose products are involved in the TCA cycle, including *PDA1* and *PDB1,* the E1 alpha and beta subunits of the pyruvate dehydrogenase complex (PDH). PDH converts pyruvate to acetyl-CoA, while reducing NAD + to NADH in the mitochondrion, linking the anaerobic glycolysis of sugars to the aerobic tricarboxylic acid cycle. Although it has been shown previously that *LPD1,* encoding the E3

component of PDH, and *PDX1,* encoding an essential component of the PDH complex, are involved in *C. albicans* filamentation [39,40], the role of *PDA1* and *PDB1* in *C. albicans* in either filamentation or biofilm formation is not known. Here, we studied the effect of overexpression of *PDA1* and *PDB1* on *C. albicans* biofilm formation and filamentation. We showed that *PDB1* overexpression specifically affects filamentation on solid surfaces without a significant effect in liquid medium. Further, it impairs mitochondrial activity as revealed by TTC assay. Tao et al. (2017) have reported the involvement of the TCA cycle in the regulation of CO_2 sensing and *C. albicans* hyphal development [41]. They observed a compromised hyphal formation with the null mutants of some of the genes encoding enzymes involved in the TCA cycle, namely *KGD2*, *SDH2*, *SDH3* and *MDH1-1*, in the presence of 5% CO_2. The authors suggested this occurs through the use of ATP, as the ATP cycle integrates with the Ras1-cAMP signaling pathway, which is a central regulator of the hyphal development. In another study, Huang et al. (2017) have highlighted the role of Nuo2, a subunit of the *C. albicans* mitochondrial complex I, in hyphal growth and biofilm formation when the carbon source is mannitol [42]. Therefore, mitochondrial activity is critical for filamentation and biofilm-forming behavior of *C. albicans.* In this study, we have shown that overexpression of *PDB1* leads to a compromised mitochondrial activity, as evidenced by TTC assay, which resulted in filamentation defect during growth on solid surfaces. As filamentation plays a crucial role during *C. albicans* biofilm establishment, it is likely that the biofilm reduction observed upon overexpression of *PDB1* is a mere consequence of the filamentation defect observed in this condition. However, whether the defects in filamentation and biofilm formation are linked to the PDH activity or to a specific role of Pdb1 in *C. albicans* filamentation remains to be determined.

Taken together, this study pinpoints remodeling of cellular metabolism as a major event of the *C. albicans* biofilm formation and provides a robust information about *C. albicans* biofilm differentially expressed genes and the altered pathways.

4. Materials and methods

4.1. Data availability

Genome-wide expression data have been deposited to European Nucleotide Archive (ENA) under the accession number E-MTAB-11383.

4.2. Media and condition

C. albicans strains were grown in YPD (1% yeast extract, 2% peptone and 2% dextrose) at 30 °C for planktonic growth and at 37 °C for biofilm growth. Filamentation assays were performed at 37 °C in YPD supplemented with 20% Fetal Bovine Serum. Solid media were obtained by adding 2% agar.

4.3. Strain construction

ORF19.3097, *ORF19.4602*, *ORF19.5211*, *ORF19.5791*, *ORF19.3358*, *ORF19.2525*, *ORF19.6126* and *ORF19.5294* were PCR amplified from *C. albicans* SC5314 genomic DNA using primers 33_A04_for and 33_A04_rev, 25_H05_for and 25_H05_rev, 35_E06_for and 35_E06_rev, 29_H02_for and 29_H02_rev, 24_H06_for and 24_H06_rev, 30_E08_for and 30_E08_rev, 36_B10_for and 36_B10_rev and 30_H03_for and 30_H03_rev, respectively (Supplementary Table 1), and Invitrogen Taq Polymerase. PCR conditions were as follows: 94 °C for 3 min, then 27 cycles at 94 °C for 30 s, 50 °C for 30s, and 72 °C for 1−3 min according to the ORF size, followed by an extension step at 72 °C for 5 min. The resulting

PCR products were checked by agarose gel electrophoresis, ethanol precipitated and resuspended in water. They were then mixed with the donor plasmid pDONR207 (Invitrogen), and subjected to a recombination reaction with Invitrogen Gateway BP Clonase™, as described (Legrand et al., 2018), to yield Entry vectors. The recombination mixes were transformed into *E. coli* Top10 and one transformant per ORF was selected for further study. The cloned ORFs were sequenced to ascertain that no mutations were introduced during PCR amplification.

The Entry plasmids were used in a Gateway™ LR reaction together with the CIp10-P$_{TET}$-GTW vector [43]. The recombination mixes were transformed into *E. coli* Top10 and one transformant was used for plasmid preparation. BsrGI digestion was used to verify the cloning of the appropriate ORF. The expression plasmids were digested by StuI prior to transformation into *C. albicans* strain CEC4642. Transformants were selected for prototrophy and proper integration at the *RPS1* locus verified by PCR using CIpUL and CIpUR primers as [32].

4.4. In vitro *biofilm formation and dry biomass measurement*

Biofilm assays were performed directly on the bottom of 12 well polystyrene plates or silicone squares in 2 ml of YPD medium. The plates were inoculated with 2 ml of cells at OD600 = 0.2 and incubated at 37 °C for 60 min at 110 rpm agitation for initial adhesion of the cells. After 60 min, the plates were washed with 2 ml of 1× PBS, and 2 ml of fresh YPD medium was added. Plates were then sealed with Breathseal sealing membranes (Greiner bio-one) and incubated at 37 °C for 18 h to form biofilms. The medium was aspirated and the wells were gently washed with 1× PBS. To estimate the dry biomass of biofilms, biofilms were scrapped and the content of each well was transferred to pre-weighed nitrocellulose filters. Biofilm-containing filters were dried overnight at 60 °C and weighed. The average total biomass for each strain was calculated from three independent samples after subtracting the mass of the empty filter.

4.5. CLSM for biofilm imaging

Biofilms grown on the surface of silicone squares in YPD medium for 18 h were gently washed with 1× PBS and stained with 50 µg/ml of concanavalin A-Alexa Fluor 594 (Invitrogen, C-11253) for 2 h at 110 rpm. Silicone squares were then placed in a Petri dish, and biofilms were covered with 1× PBS. Biofilms were imaged as described previously [20]: CSLM was performed at the UtechS PBI facility of Institut Pasteur using an upright LSM700 microscope equipped with a Zeiss 40×/1.0 W plan-Apochromat immersion objective. Images were acquired and assembled into maximum intensity Z-stack projection using the ZEN software.

4.6. RNA extraction

RNA was isolated from *C. albicans* strains (CEC4665) with the RNeasy mini kit mirVana RNA isolation kit (Cat. No. 74104, Qiagen). Briefly, *C. albicans* planktonic and biofilm cells were grown in YPD medium. Total RNA was isolated from four independent wild-type planktonic and biofilm cultures. Planktonic cells were grown in YPD medium at 30 °C till OD600 = 0.8 whereas biofilm was grown in YPD medium at 37 °C for 18 h. Cells were pelleted down at 4000 rpm, washed 3 times with 1× PBS, and resuspended in 700 µl of extraction buffer. Cells were broken in a bead-beater with 500 µl of 0.5 mm of glass beads (six cycles of 2 min at 10). RNeasy columns were used to isolate total RNA. To remove the potential contaminating chromosomal DNA, RNA samples were treated on-column with DNAse for 15 min at room temperature (Cat. No. 79254, Qiagen).

4.7. RNA sequencing and analysis

Libraries were built using a TruSeq Stranded mRNA library Preparation Kit (Illumina, USA) following the manufacturer's protocol. Quality control was performed on an Agilent BioAnalyzer. RNA sequencing was performed on the Illumina NextSeq 500 platform using single-end 75bp. The RNA-seq analysis was performed with Sequana [44]. We used the RNA-seq pipeline (v0.9.16, https://github.com/sequana/sequana_rnaseq) built on top of Snakemake 5.8.1 [45]. Reads were trimmed from adapters using Cutadapt 2.10 [46] then mapped to the *C. albicans* (SC5314, version A22-s07-m01-r105) genome assembly and annotation from *Candida* Genome Database [47] using STAR 2.7.3a [48]. FeatureCounts 2.0.0 [49] was used to produce the count matrix, assigning reads to features with strand-specificity information. Quality control statistics were summarized using MultiQC 1.8 [50]. Statistical analysis on the count matrix was performed to identify differentially regulated genes, comparing biofilm and planktonic condition RNA expression. Clustering of transcriptomic profiles were assessed using a Principal Component Analysis (PCA). Differential expression testing was conducted using DESeq2 library 1.24.0 [51] scripts based on SARTools 1.7.0 [52] indicating the significance (Benjamini-Hochberg adjusted *p*-values, false discovery rate FDR < 0.05) and the effect size (fold-change) for each comparison. Functional categorization of up-and down-regulated genes were achieved by using FungiFun2 [53].

4.8. Filamentation assay

The filamentation assays were performed with YPD medium containing 20% fetal bovine serum with or without 40 μg/ml doxycycline. Strains grown overnight in YPD medium were spotted on the plate and incubated for 3 days at 37 °C. Filamentation was examined at the colony level by plating dilution of overnight cultures on YPD medium containing 20% fetal bovine serum. The plates were incubated for 5 days at 37 °C and photographed using a PhenoBooth (Singer Instruments).

4.9. Growth kinetics

Strains grown overnight in YPD with or without 40 μg/ml doxycycline at 30 °C were inoculated in a 96-well microtiter plate at a final OD600 = 0.1 in 200 μl YPD supplemented with or without 40 μg/ml doxycycline. Growth at 30 °C was monitored every 30 min using a microplate reader (TECAN Sunrise). Growth curves were performed in triplicate.

4.10. TTC assay

To analyze the respiratory activity, *C. albicans* strains were spotted on YPD plates and incubated 24h at 30 °C. Then 0.025% TTC in 1%agarose solution was poured on the top of the plates and incubated for 30 min at room temperature and photographed using Phenobooth.

Declaration of competing interest

No conflict of interest.

Acknowledgments

Appendix A. Supplementary data

Supplementary data to this article can be found online at https://doi.org/10.1016/j.resmic.2022.104014.

References

[1] Costerton JW, Cheng KJ, Geesey GG, Ladd TI, Nickel JC, Dasgupta M, et al. Bacterial biofilms in nature and disease. Annu Rev Microbiol 1987;41:435−64. https://doi.org/10.1146/annurev.mi.41.100187.002251.

[2] Kolter R. Biofilms in lab and nature: a molecular geneticist's voyage to microbial ecology. Int Microbiol Off J Span Soc Microbiol 2010;13:1−7. https://doi.org/10.2436/20.1501.01.105.

[3] López D, Vlamakis H, Kolter R. Biofilms. Cold Spring Harb Perspect Biol 2010;2:a000398. https://doi.org/10.1101/cshperspect.a000398.

[4] Kumamoto CA, Vinces MD. Alternative *Candida* lifestyles: growth on surfaces. Annu Rev Microbiol 2005;59:113−33. https://doi.org/10.1146/annurev.micro.59.030804.121034.

[5] Achkar JM, Fries BC. *Candida* infections of the genitourinary tract. Clin Microbiol Rev 2010;23:253−73. https://doi.org/10.1128/cmr.00076-09.

[6] Ganguly S, Mitchell AP. Mucosal biofilms of *Candida albicans*. Curr Opin Microbiol 2011;14:380−5. https://doi.org/10.1016/j.mib.2011.06.001.

[7] Chandra J, Kuhn DM, Mukherjee PK, Hoyer LL, McCormick T, Ghannoum MA. Biofilm Formation by the fungal pathogen *Candida albicans*: development, architecture, and drug resistance. J Bacteriol 2001;183:5385−94. https://doi.org/10.1128/jb.183.18.5385-5394.2001.

[8] Ramage G, Mowat E, Jones B, Williams C, Lopez-Ribot J. Our current understanding of fungal biofilms. Crit Rev Microbiol 2009;35:340−55. https://doi.org/10.3109/10408410903241436.

[9] Nobile CJ, Johnson AD. *Candida albicans* biofilms and human disease. Annu Rev Microbiol 2015;69:71−92. https://doi.org/10.1146/annurev-micro-091014-104330.

[10] Finkel JS, Mitchell AP. Genetic control of *Candida albicans* biofilm development. Nat Rev Microbiol 2011;9:109. https://doi.org/10.1038/nrmicro2475.

[11] Fanning S, Mitchell AP. Fungal biofilms. PLoS Pathog 2012;8:e1002585. https://doi.org/10.1371/journal.ppat.1002585.

[12] Mathé L, Dijck PV. Recent insights into *Candida albicans* biofilm resistance mechanisms. Curr Genet 2013;59:251−64. https://doi.org/10.1007/s00294-013-0400-3.

[13] Gulati M, Nobile CJ. *Candida albicans* biofilms: development, regulation, and molecular mechanisms. Microb Infect 2016;18:310−21. https://doi.org/10.1016/j.micinf.2016.01.002.

[14] Pierce CG, Vila T, Romo JA, Montelongo-Jauregui D, Wall G, Ramasubramanian A, et al. The *Candida albicans* biofilm matrix: composition, structure and function. J Fungi 2017;3:14. https://doi.org/10.3390/jof3010014.

[15] Douglas LJ. *Candida* biofilms and their role in infection. Trends Microbiol 2003;11:30−6. https://doi.org/10.1016/s0966-842x(02)00002-1.

[16] Uppuluri P, Chaturvedi AK, Srinivasan A, Banerjee M, Ramasubramaniam AK, Köhler JR, et al. Dispersion as an important step in the *Candida albicans* biofilm developmental cycle. PLoS Pathog 2010;6:e1000828. https://doi.org/10.1371/journal.ppat.1000828.

[17] Andes D, Nett J, Oschel P, Albrecht R, Marchillo K, Pitula A. Development and characterization of an in vivo central venous catheter *Candida albicans* biofilm model. Infect Immun 2004;72:6023−31. https://doi.org/10.1128/iai.72.10.6023-6031.2004.

[18] Nett J, Andes D. *Candida albicans* biofilm development, modeling a host−pathogen interaction. Curr Opin Microbiol 2006;9:340−5. https://doi.org/10.1016/j.mib.2006.06.007.

[19] Nett JE, Crawford K, Marchillo K, Andes DR. Role of Fks1p and matrix glucan in *Candida albicans* biofilm resistance to an echinocandin, pyrimidine, and polyene. Antimicrob Agents Chemother 2010;54:3505−8. https://doi.org/10.1128/aac.00227-10.

[20] Nobile CJ, Mitchell AP. Regulation of cell-surface genes and biofilm formation by the *C. albicans* transcription factor Bcr1p. Curr Biol 2005;15:1150−5. https://doi.org/10.1016/j.cub.2005.05.047.

[21] Sellam A, Tebbji F, Nantel A. Role of Ndt80p in sterol metabolism regulation and azole resistance in *Candida albicans*. Eukaryot Cell 2009;8:1174−83. https://doi.org/10.1128/ec.00074-09.

[22] Daniels KJ, Park Y-N, Srikantha T, Pujol C, Soll DR. Impact of environmental conditions on the form and function of *Candida albicans* biofilms. Eukaryot Cell 2013;12:1389−402. https://doi.org/10.1128/ec.00127-13.

[23] Rai LS, Singha R, Sanchez H, Chakraborty T, Chand B, Bachellier-Bassi S, et al. The *Candida albicans* biofilm gene circuit modulated at the chromatin level by a recent molecular histone innovation. PLoS Biol 2019;17:e3000422. https://doi.org/10.1371/journal.pbio.3000422.

[24] Bonhomme J, Chauvel M, Goyard S, Roux P, Rossignol T, d'Enfert C. Contribution of the glycolytic flux and hypoxia adaptation to efficient biofilm

formation by *Candida albicans*. Mol Microbiol 2011;80:995–1013. https://doi.org/10.1111/j.1365-2958.2011.07626.x.

[25] Nobile CJ, Fox EP, Nett JE, Sorrells TR, Mitrovich QM, Hernday AD, et al. A recently evolved transcriptional network controls biofilm development in *Candida albicans*. Cell 2012;148:126–38. https://doi.org/10.1016/j.cell.2011.10.048.

[26] García-Sánchez S, Aubert S, Iraqui I, Janbon G, Ghigo J-M, d'Enfert C. *Candida albicans* biofilms: a developmental state associated with specific and stable gene expression patterns. Eukaryot Cell 2004;3:536–45. https://doi.org/10.1128/ec.3.2.536-545.2004.

[27] Yeater KM, Chandra J, Cheng G, Mukherjee PK, Zhao X, Rodriguez-Zas SL, et al. Temporal analysis of *Candida albicans* gene expression during biofilm development. Microbiology 2007;153:2373–85. https://doi.org/10.1099/mic.0.2007/006163-0.

[28] Huang MY, Woolford CA, May G, McManus CJ, Mitchell AP. Circuit diversification in a biofilm regulatory network. PLoS Pathog 2019;15:e1007787. https://doi.org/10.1371/journal.ppat.1007787.

[29] Zhu Z, Wang H, Shang Q, Jiang Y, Cao Y, Chai Y. Time course analysis of *Candida albicans* metabolites during biofilm development. J Proteome Res 2013;12:2375–85. https://doi.org/10.1021/pr300447k.

[30] Rajendran R, May A, Sherry L, Kean R, Williams C, Jones BL, et al. Integrating *Candida albicans* metabolism with biofilm heterogeneity by transcriptome mapping. Sci Rep 2016;6:35436. https://doi.org/10.1038/srep35436.

[31] Desai JV, Mitchell AP. *Candida albicans* biofilm development and its genetic control. Microbiol Spectr 2015;3. https://doi.org/10.1128/microbiolspec.mb-0005-2014. 10.1128/microbiolspec.MB-0005–2014.

[32] Legrand M, Bachellier-Bassi S, Lee KK, Chaudhari Y, Tournu H, Arbogast L, et al. Generating genomic platforms to study *Candida albicans* pathogenesis. Nucleic Acids Res 2018;46:6935–49. https://doi.org/10.1093/nar/gky594.

[33] Rai LS, Wijlick LV, Bougnoux M, Bachellier-Bassi S, d'Enfert C. Regulators of Commensal and Pathogenic Life-styles of an Opportunistic Fungus - *Candida albicans*. Yeast 2021. https://doi.org/10.1002/yea.3550.

[34] Rich PR, Mischis LA, Purton S, Wiskich JT. The sites of interaction of triphenyltetrazolium chloride with mitochondrial respiratory chains. Fems Microbiol Lett 2001;202:181–7. https://doi.org/10.1111/j.1574-6968.2001.tb10801.x.

[35] Pisithkul T, Schroeder JW, Trujillo EA, Yeesin P, Stevenson DM, Chaiamarit T, et al. Metabolic remodeling during biofilm development of *Bacillus subtilis*. mBio 2019;10:006233-e719. https://doi.org/10.1128/mbio.00623-19.

[36] Böttcher B, Driesch D, Krüger T, Garbe E, Gerwien F, Kniemeyer O, et al. Impaired amino acid uptake leads to global metabolic imbalance of *Candida albicans* biofilms. Npj Biofilms Microbiomes 2022;8:78. https://doi.org/10.1038/s41522-022-00341-9.

[37] Fox EP, Cowley ES, Nobile CJ, Hartooni N, Newman DK, Johnson AD. Anaerobic bacteria grow within *Candida albicans* biofilms and induce biofilm formation in suspension cultures. Curr Biol 2014;24:2411–6. https://doi.org/10.1016/j.cub.2014.08.057.

[38] Rossignol T, Ding C, Guida A, d'Enfert C, Higgins DG, Butler G. Correlation between biofilm formation and the hypoxic response in *Candida parapsilosis*. Eukaryot Cell 2009;8:550–9. https://doi.org/10.1128/ec.00350-08.

[39] Vellucci VF, Gygax SE, Hostetter MK. Involvement of *Candida albicans* pyruvate dehydrogenase complex protein X (Pdx1) in filamentation. Fungal Genet Biol 2007;44:979–90. https://doi.org/10.1016/j.fgb.2006.12.003.

[40] Kim S-Y, Kim J. Roles of dihydrolipoamide dehydrogenase Lpd1 in *Candida albicans* filamentation. Fungal Genet Biol 2010;47:782–8. https://doi.org/10.1016/j.fgb.2010.06.005.

[41] Tao L, Zhang Y, Fan S, Nobile CJ, Guan G, Huang G. Integration of the tricarboxylic acid (TCA) cycle with cAMP signaling and Sfl2 pathways in the regulation of CO_2 sensing and hyphal development in *Candida albicans*. PLoS Genet 2017;13:e1006949. https://doi.org/10.1371/journal.pgen.1006949.

[42] Huang X, Chen X, He Y, Yu X, Li S, Gao N, et al. Mitochondrial complex I bridges a connection between regulation of carbon flexibility and gastrointestinal commensalism in the human fungal pathogen *Candida albicans*. PLoS Pathog 2017;13:e1006414. https://doi.org/10.1371/journal.ppat.1006414.

[43] Chauvel M, Nesseir A, Cabral V, Znaidi S, Goyard S, Bachellier-Bassi S, et al. A versatile overexpression strategy in the pathogenic yeast *Candida albicans*: identification of regulators of morphogenesis and fitness. PLoS One 2012;7:e45912. https://doi.org/10.1371/journal.pone.0045912.

[44] Cokelaer T, Desvillechabrol D, Legendre R, Cardon M. 'Sequana': a set of Snakemake NGS pipelines. J Open Source Softw 2017;2:352. https://doi.org/10.21105/joss.00352.

[45] Köster J, Rahmann S. Snakemake—a scalable bioinformatics workflow engine. Bioinformatics 2012;28:2520–2. https://doi.org/10.1093/bioinformatics/bts480.

[46] Martin M. Cutadapt removes adapter sequences from high-throughput sequencing reads. EMBnetJournal 2011;17:10–2. https://doi.org/10.14806/ej.17.1.200.

[47] Skrzypek MS, Binkley J, Binkley G, Miyasato SR, Simison M, Sherlock G. The *Candida* Genome Database (CGD): incorporation of Assembly 22, systematic identifiers and visualization of high throughput sequencing data. Nucleic Acids Res 2017;45:D592–6. https://doi.org/10.1093/nar/gkw924.

[48] Dobin A, Davis CA, Schlesinger F, Drenkow J, Zaleski C, Jha S, et al. STAR: ultrafast universal RNA-seq aligner. Bioinformatics 2013;29:15–21. https://doi.org/10.1093/bioinformatics/bts635.

[49] Liao Y, Smyth GK, Shi W. featureCounts: an efficient general purpose program for assigning sequence reads to genomic features. Bioinformatics 2014;30:923–30. https://doi.org/10.1093/bioinformatics/btt656.

[50] Ewels P, Magnusson M, Lundin S, Käller M. MultiQC: summarize analysis results for multiple tools and samples in a single report. Bioinformatics 2016;32:3047–8. https://doi.org/10.1093/bioinformatics/btw354.

[51] Love MI, Huber W, Anders S. Moderated estimation of fold change and dispersion for RNA-seq data with DESeq2. Genome Biol 2014;15:550. https://doi.org/10.1186/s13059-014-0550-8.

[52] Varet H, Brillet-Guéguen L, Coppée J-Y, Dillies M-A. SARTools: a DESeq2- and EdgeR-based R pipeline for comprehensive differential analysis of RNA-seq data. PLoS One 2016;11:e0157022. https://doi.org/10.1371/journal.pone.0157022.

[53] Priebe S, Kreisel C, Horn F, Guthke R, Linde J. FungiFun2: a comprehensive online resource for systematic analysis of gene lists from fungal species. Bioinformatics 2015;31:445–6. https://doi.org/10.1093/bioSinformatics/btu627.